American Mineralogist, Volume 77, pages 945–953, 1992

Crystal chemistry of vesuvianite: Site preferences of square-pyramidal coordinated sites

Makio Ohkawa, Akira Yoshiasa, Setsuo Takeno
Faculty of Science, Hiroshima University, Higashi-Hiroshima 724, Japan

Abstract

The crystal structures of four vesuvianite crystals (three from Japan and one from Norway) were refined by single-crystal X-ray diffraction. All four crystals have space group $P4/nnc$ and have the following cell parameters (Å): a = 15.517(6), 15.606(4), 15.583(18), 15.546(23); c = 11.781(4), 11.825(4), 11.801(17), 11.828(14), respectively. The final R indices for 1414, 1498, 1363, and 1337 observed reflections are 0.031, 0.033, 0.040, and 0.068, respectively. The EXAFS method was also used to investigate the local environment of the Cu and Mn ions in vesuvianite from Sauland, Norway, and Nakatatsu mine, Japan.

The local structures and site preferences of ions along the fourfold rotation axis were examined in detail. Based on site-population refinements and observed cation-anion interatomic distances obtained by X-ray single-crystal diffraction and EXAFS methods, the fivefold-coordinated B site is determined to be occupied by Mn^{2+}, Fe^{2+}, Fe^{3+}, Cu^{2+}, and Mg^{2+}. This site was also found to be larger than the octahedral A and AlFe sites and more variable in size, reflecting the ionic radius of the occupying cations. The correlation between B-O10 and O10-O10 distances leads to the following conclusions: (1) when the B site is occupied by large ions such as Fe^{2+} and Mn^{2+}, the O10 site prefers F, which has a smaller ionic radius than that of O; (2) the size of the B site varies with the displacement of the O10 atoms along the fourfold rotation axes and also with the displacement of the B site itself; (3) the displacements of the F ions in the O10 site along the fourfold rotation axes are greater than that of O ions because no H bonds exist between the F atoms.

Introduction

Vesuvianite (idocrase) commonly occurs in skarn and rarely in metamorphic and igneous rocks. The crystal structure of vesuvianite was first determined by Warren and Modell (1931) on the basis on the structural similarities between cubic grossular garnet and tetragonal vesuvianite. The structure of vesuvianite around the fourfold rotoinversion axis is closely related to that of grossular garnet; the c axis of vesuvianite is approximately equal in length to the cube edge of grossular. In fact, the two minerals often coexist intimately in nature (e.g., Deer et al., 1982). Coda et al. (1970) and Rucklidge et al. (1975) revised the distribution of atoms along the fourfold rotation axis of the structural model proposed by Warren and Modell (1931). Yoshiasa and Matsumoto (1986) investigated site preferences of cations and OH groups in vesuvianite and proposed the chemical formula for the one-half unit cell as $Ca_{19}(Mn,Fe^{2+})(F,OH)_2(Mg,Fe^{2+},Mn,Al,Fe^{3+},Ti)_8Al_4(OH,F,O)_8(SiO_4)_{10}(Si_2O_7)_4$.

The crystal structure of vesuvianite is chiefly characterized by the atomic arrangement along the fourfold rotation axis. Atoms arranged along this axis are not connected directly to the grossular-like structure. Two anion and four cation positions are arranged along the fourfold rotation axis. Two fivefold- and two eightfold-coordinated cation positions are statistically half occupied by one Fe and one Ca ion, respectively (Coda et al., 1970; Rucklidge et al., 1975). These fivefold and eightfold sites are labeled B and C, respectively, in this paper, in accordance with Rucklidge et al. (1975). It should be emphasized that the adjacent B and C positions are not occupied together because of their close arrangement (i.e., only one of each is fully occupied). Furthermore, Coda et al. (1970) pointed out the close arrangement of the C sites, and Giuseppetti and Mazzi (1983) suggested the impossibility of the C polyhedra sharing a face. Consequently, the site occupancy ratio of B:C is 1:1. However, this has not been confirmed experimentally. Giuseppetti and Mazzi (1983) and Fitzgerald et al. (1986b) have noted that the ordering of the two ions in the statistically occupied B and C sites along the fourfold rotation axis causes a decrease in the symmetry from that of space group $P4/nnc$.

In the vesuvianite structure, only O10 and O11 are not bonded to Si ions. Coda et al. (1970) suggested that the two sites are probably associated with H atoms. More recently, Yoshiasa and Matsumoto (1986) determined a likely position for the H atom bonded to O11, but that of O10 remains to be determined because O10 is entirely occupied by F in their vesuvianite sample. Lager et al. (1989) determined the H atom positions by neutron diffraction methods.

As described above, several important problems such as the site preferences, the cation occupancy ratio of sites B and C, and the substitution of OH by F have not been established for vesuvianite. These problems are gradually

0003–004X/92/0910–0945$02.00

TABLE 1. Microprobe analyses for the vesuvianite samples studied

	1 Sauland	2 Sanpo	3 Jinmu	4 Chichibu
Oxide	**wt%**			
SiO_2	37.18	36.16	36.97	36.92
TiO_2	0.05	1.83	0.03	0.32
Al_2O_3	19.33	15.48	17.75	17.03
FeO	0.20	4.82	4.15	2.72
MnO	0.16	0.21	0.55	0.02
MgO	1.80	1.68	1.22	3.30
CaO	36.54	35.39	36.31	36.87
Na_2O	0.13	0.02	0.06	0.01
K_2O	0.01	0.01	0.0	0.02
CuO	1.01	—	—	—
F	1.59	1.29	1.40	0.05
H_2O_{calc}	2.34	2.40	2.42	3.08
$-O = F$	0.67	0.55	0.59	0.02
Total	99.68	98.74	100.28	100.32
	Number of atoms (moles per 50 cations)			
Si	18.02	18.00	18.00	17.75
Ti	0.02	0.68	0.01	0.12
Al	11.04	9.08	10.19	9.65
Fe	0.08	2.01	1.69	1.09
Mn	0.07	0.09	0.23	0.01
Mg	1.30	1.25	0.88	2.36
Ca	18.98	18.87	18.94	19.00
Na	0.13	0.02	0.06	0.01
K	0.0	0.01	0.0	0.01
Cu	0.37	—	—	—
F	2.44	2.04	2.16	0.08

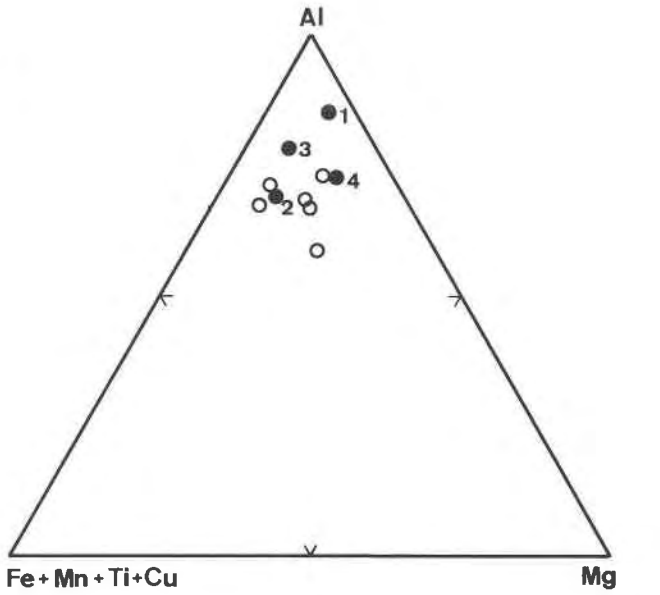

Fig. 2. Vesuvianite compositions plotted on an AFM diagram (atomic proportions Al-Fe + Mn + Ti + Cu-Mg). Specimen numbers are the same as those in Table 1.

being resolved using recently developed techniques (e.g., Giuseppetti and Mazzi, 1983; Valley et al., 1985; Yoshiasa and Matsumoto, 1986; Fitzgerald et al., 1986a, 1986b, 1987; Phillips et al., 1987).

In this study, the site preferences of ions in the B and C sites and in the O10 site for F along the fourfold rotation axis and the local structure around the B sites are examined in detail.

EXPERIMENTAL

Specimens used

Chemical analyses (11 elements) were obtained for nine Japanese vesuvianite samples (from Chichibu mine in Saitama Prefecture, Nakatatsu mine in Fukui Prefecture, Sanpo mine and Tetta in Okayama Prefecture, Jinmu mine and Tojyo in Hiroshima Prefecture, Yawatahama in Ehime Prefecture, and Obira and Kiura mines in Oita Prefecture) and a copper vesuvianite sample from Sauland, Telemark, Norway (Neumann and Svinndal, 1955; Ito and Arem, 1970), using the JCMA-733II electron microprobe analyzer. Several points on each sample were analyzed, and the four representative analyses, upon which the crystal-structure determinations were based, are presented in Table 1. Table 1 also shows the number of ions calculated from the analytical data assuming 50 cations per half of the unit cell. In the calculation, all Fe ions were assumed to be present in the divalent state. Chemical compositions of the ten specimens are plotted in ACF and AFM diagrams (Figs. 1a, 2). In Figure 2, the four specimens used for structure analyses are represented by the solid circles.

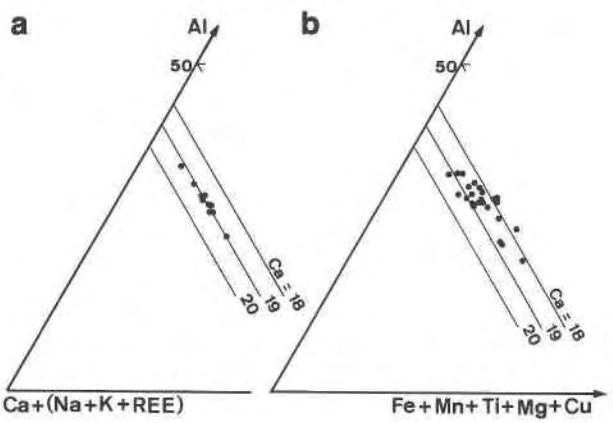

Fig. 1. Vesuvianite compositions [(a) this study, (b) data from Deer et al. (1982)] plotted on an ACF diagram [atomic proportions Al-Ca + (Na + K)-Fe + Mn + Ti + Mg + Cu]. Lines indicate the number of Ca ions per formula unit.

The copper vesuvianite from Sauland (specimen 1) and three Japanese specimens (specimen 2 from Sanpo mine, specimen 3 from Jinmu mine, and specimen 4 from Chichibu mine) were chosen for structural analyses for the following reasons: specimen 1 was chosen in order to determine the site preference of the Cu ion, specimen 2 to investigate the possibility of lower symmetry (the existence of forbidden reflections was suggested by Chiyoko Henmi, Okayama University, on the basis of Weissenberg photographs; personal communication), specimen 3 because of its intermediate composition among the selected four specimens, and specimen 4 because of its small F content (see Fig. 2 and Table 1). The last three specimens are from skarn deposits. Colors and habits are blue and acicular (specimen 1), brown and acicular (specimen

TABLE 2. Crystal and refinement data

	1 Sauland	2 Sanpo	3 Jinmu	4 Chichibu
a (Å)	15.517(6)	15.606(4)	15.583(18)	15.546(23)
c	11.781(4)	11.825(4)	11.801(17)	11.828(14)
V (Å^3)	2836.4	2880.1	2865.6	2858.6
Space group	$P4/nnc$			
D_{calc} (g/cm^3)	3.37	3.39	3.38	3.36
Radiation used	Mo$K\alpha$ (0.71069 Å)			
Monochromator	graphite			
Crystal size (mm)	0.16 sphere	0.18 sphere	0.16 × 0.13 × 0.11	0.23 sphere
μ(Mo$K\alpha$) (cm^{-1})	25.79	29.31	28.26	26.58
Diffractometer	Rigaku AFC-5			
Scan type	ω			
2θ range (°)	1–55			
Meas. refl.	3681	3773	3704	3696
Indepen. refl. with $F_o > 3\sigma(F_o)$	1414	1498	1363	1337
R (%)	3.1	3.3	4.0	6.8
R_w (%)	3.5	3.9	3.7	7.8

2), green and acicular (specimen 3), and green and massive (specimen 4).

Structure analyses

Three specimens were ground into spheres. Specimen 3 was not ground because of its small crystal size. These samples were mounted on fine glass capillaries. The intensity data were obtained using a Rigaku AFC-5 four-circle diffractometer with graphite-monochromatized Mo$K\alpha$ radiation (50 kV, 160 mA) and were corrected for Lorentz and polarization factors. No absorption corrections were made because of small μr values (0.21, 0.26, 0.20, and 0.31 for specimens 1–4, respectively). The systematic absences ($hk0$ refections are present only with $h + k = 2n$, $h0l$ with $h + l = 2n$, and hhl with $l = 2n$) were consistent with space group $P4/nnc$. Equivalent reflections were averaged. Coincidence factors were 0.016, 0.017, 0.033, and 0.031, respectively. Scattering factors of neutral atoms were taken from *International Tables for X-ray Crystallography* (Ibers and Hamilton, 1974). Anomalous dispersion corrections were made for all atoms. The refinement was initiated with the positional parameters reported by Yoshiasa and Matsumoto (1986) using the program RFINE 2 (Finger, 1969). Table 2 lists crystal and refinement data.

Site assignments and terminology were based on the model of Rucklidge et al. (1975). After several cycles of refinements, total site occupancy factors were constrained to 1.0 (statistically half-occupied B and C sites were constrained to 0.5), and site assignments were modified as consistent with chemical analyses. H atom positions were not included in the refinement models. Refined occupancy factors for each site are shown in Table 3.

The refined positional parameters and thermal parameters are listed in Tables 4 and 5,[1] respectively. The calculated cation-anion interatomic distances are given in Table 6. Observed and calculated structure factors are listed in Table 7.

EXAFS method

Specimen 1 and the vesuvianite from the Nakatatsu mine were analyzed by EXAFS to obtain information on the local structure around Cu and Mn ions. The crystal structure of the latter was previously studied by Yoshiasa and Matsumoto (1986).

Both vesuvianite samples were ground into a powder and pressed with powdered boron nitride into pellets of 10.0-mm diameter and suitable thickness. The X-ray absorption measurements near the Cu and MnK edge were made with synchrotron radiation at the Photon Factory facilities, Tsukuba. The EXAFS interference function was extracted from the measured absorption data using standard techniques (Maeda, 1987). The Fourier transform of the EXAFS interference function to real space yields a radial structure function. The Fourier transforms for the Cu and MnK edges are shown in Figure 3, with no phase shift correction. The high-frequency noise and the small residual background in each spectrum were removed by a Fourier filtering technique. The Fourier-filtered EXAFS data were fitted using the least-squares minimization technique with an analytical EXAFS formula. The backscattering amplitude of photoelectrons and the phase shift

TABLE 3. Refined occupancy factors

	1 Sauland	2 Sanpo	3 Jinmu	4 Chichibu
Ca1-Ca3	Ca 1.0			
C	Ca 0.5			
B	Cu 0.26(1)	Fe 0.5	Fe 0.5	Mg 0.26(1)
	Mg 0.24			Fe 0.24
AlFe	Mg 0.14	Al 0.81(1)	Al 0.87(1)	Al 0.97(1)
	Al 0.86(11)	Fe 0.19	Fe 0.13	Fe 0.03
A	Al 1.0			
Si1-Si3	Si 1.0			
O1-O9	O 1.0			
O10	O 0.42		O 0.09	O 1.0
	F 0.58(10)	F 1.0	F 0.91(13)	
O11	O 0.47	O 1.0	O 0.46	O 1.0
	F 0.53(4)		F 0.54(6)	

[1] To receive a copy of Tables 5, 6, and 7, order Document AM-92-505 from the Business Office, Mineralogical Society of America, 1130 Seventeenth Street NW, Suite 330, Washington, DC 20036, U.S.A. Please remit $5.00 in advance for the microfiche.

Table 4. Positional parameters for vesuvianite

	1 Sauland (copper vesuvianite)				2 Sanpo		
Atom	*x*	*y*	*z*	Atom	*x*	*y*	*z*
Ca1	−¼	¼	¼	Ca1	−¼	¼	¼
Ca2	−0.1891(1)	0.0443(1)	0.3795(1)	Ca2	−0.1890(1)	0.0437(1)	0.3795(1)
Ca3	−0.1015(1)	−0.1802(1)	0.8882(1)	Ca3	−0.0986(1)	−0.1785(1)	0.8855(1)
C	−¼	−¼	0.1428(2)	C	−¼	−¼	0.1355(3)
B	−¼	−¼	0.0543(2)	B	−¼	−¼	0.0564(3)
AlFe	−0.1124(1)	0.1211(1)	0.1265(1)	AlFe	−0.1118(1)	0.1205(1)	0.1270(1)
A	0	0	0	A	0	0	0
Si1	−¼	¼	0	Si1	−¼	¼	0
Si2	−0.1810(1)	0.0406(1)	0.8709(1)	Si2	−0.1808(1)	0.0402(1)	0.8715(1)
Si3	−0.0831(1)	−0.1508(1)	0.3648(1)	Si3	−0.0830(1)	−0.1507(1)	0.3643(1)
O1	−0.2189(1)	0.1726(1)	0.0858(2)	O1	−0.2207(1)	0.1727(1)	0.0854(2)
O2	−0.1168(1)	0.1593(1)	0.2784(2)	O2	−0.1169(1)	0.1602(1)	0.2801(2)
O3	−0.0489(1)	0.2215(1)	0.0767(2)	O3	−0.0487(1)	0.2224(1)	0.0755(2)
O4	−0.0619(1)	0.1065(1)	0.4707(2)	O4	−0.0614(1)	0.1060(1)	0.4699(2)
O5	−0.1701(1)	0.0153(2)	0.1780(2)	O5	−0.1705(1)	0.0145(2)	0.1794(2)
O6	−0.1189(2)	−0.2716(1)	0.0586(2)	O6	−0.1180(2)	−0.2712(2)	0.0598(2)
O7	0.0561(1)	0.1733(2)	0.3212(2)	O7	0.0561(1)	0.1745(2)	0.3221(2)
O8	−0.0606(1)	−0.0908(1)	0.0663(2)	O8	−0.0609(1)	−0.0904(1)	0.0666(2)
O9	−0.1447(1)	−0.1447	¼	O9	−0.1443(1)	−0.1443	¼
O10	−¼	−¼	0.8676(4)	O10	−¼	−¼	0.8515(6)
O11	−0.0046(1)	0.0625(1)	0.1362(2)	O11	−0.0040(1)	0.0618(1)	0.1357(2)
	3 Jinmu				4 Chichibu		
Atom	*x*	*y*	*z*	Atom	*x*	*y*	*z*
Ca1	−¼	¼	¼	Ca1	−¼	¼	¼
Ca2	−0.1893(1)	0.0441(1)	0.3795(1)	Ca2	−0.1892(1)	0.0449(1)	0.3794(1)
Ca3	−0.1003(1)	−0.1796(1)	0.8884(1)	Ca3	−0.1013(1)	−0.1821(1)	0.8907(2)
C	−¼	−¼	0.1410(4)	C	−¼	−¼	0.1494(6)
B	−¼	−¼	0.0555(4)	B	−¼	−¼	0.0365(6)
AlFe	−0.1123(1)	0.1209(1)	0.1267(1)	AlFe	−0.1123(1)	0.1211(1)	0.1258(2)
A	0	0	0	A	0	0	0
Si1	−¼	¼	0	Si1	−¼	¼	0
Si2	−0.1806(1)	0.0407(1)	0.8711(1)	Si2	−0.1807(1)	0.0417(1)	0.8714(2)
Si3	−0.0827(1)	−0.1506(1)	0.3645(1)	Si3	−0.0839(1)	−0.1507(1)	0.3645(2)
O1	−0.2200(2)	0.1728(2)	0.0862(3)	O1	−0.2205(3)	0.1727(3)	0.0848(4)
O2	−0.1175(2)	0.1598(2)	0.2792(3)	O2	−0.1173(3)	0.1603(3)	0.2797(5)
O3	−0.0481(2)	0.2219(2)	0.0762(3)	O3	−0.0472(3)	0.2225(3)	0.0755(4)
O4	−0.0619(2)	0.1064(2)	0.4699(2)	O4	−0.0614(3)	0.1056(3)	0.4696(4)
O5	−0.1703(2)	0.0150(2)	0.1794(3)	O5	−0.1710(3)	0.0133(4)	0.1778(5)
O6	−0.1179(2)	−0.2720(2)	0.0583(3)	O6	−0.1220(4)	−0.2734(4)	0.0573(5)
O7	0.0557(2)	0.1726(2)	0.3206(3)	O7	0.0551(3)	0.1705(4)	0.3205(5)
O8	−0.0608(2)	−0.0906(2)	0.0664(3)	O8	−0.0604(3)	−0.0909(3)	0.0671(5)
O9	−0.1447(2)	−0.1447	¼	O9	−0.1447(3)	−0.1447	¼
O10	−¼	−¼	0.8625(8)	O10	−¼	−¼	0.8657(11)
O11	−0.0035(2)	0.0616(2)	0.1360(2)	O11	−0.0035(3)	0.0609(3)	0.1363(4)

function employed here were the theoretical curves tabulated by Teo and Lee (1979). Details of the data processing procedure were given in Yoshiasa et al. (1990a, 1990b). The structural parameters around the Cu and Mn ions obtained by least-squares fitting of a fivefold one-shell model for copper vesuvianite and vesuvianite from Nakatatsu mine are listed in Table 8.

Results and discussion

Description of the structure

Figure 4 shows atomic arrangements along the fourfold rotation axis in the crystal structure of vesuvianite that are not allowed. The polyhedra around the C sites cannot share a face because of the short distance between the Ca ions (Coda et al., 1970; Giuseppetti and Mazzi, 1983). In the case where only B sites are occupied, O9 bonds only to Si3. This atomic arrangement may be a sort of defect structure and should be unstable. Occupancy of each individual B and C site is possible. Consequently, the site occupancy ratio of B:C is exactly 1:1. Figure 5 shows possible arrangements along the fourfold rotation axis. In such a crystal structure, the statistical distribution of half-occupied B and C sites yields the forbidden reflections with respect to space group $P4/nnc$. In the ACF diagram (Fig. 1a), vesuvianite compositions determined in this study concentrate near Ca = 19, and the composition is equivalent to the site occupancy ratio B:C of 1:1. Figure 1b shows variation in vesuvianite compositions taken from Deer et al. (1982). Note that most of the compositions are displaced to the Ca-poor side of Ca = 19. This may be partly due to inaccuracy in the analyses, but substitution of Ca by cations such as Mn cannot be ruled out. In any case, Ca contents of these vesuvianite samples are less than 19 per formula unit.

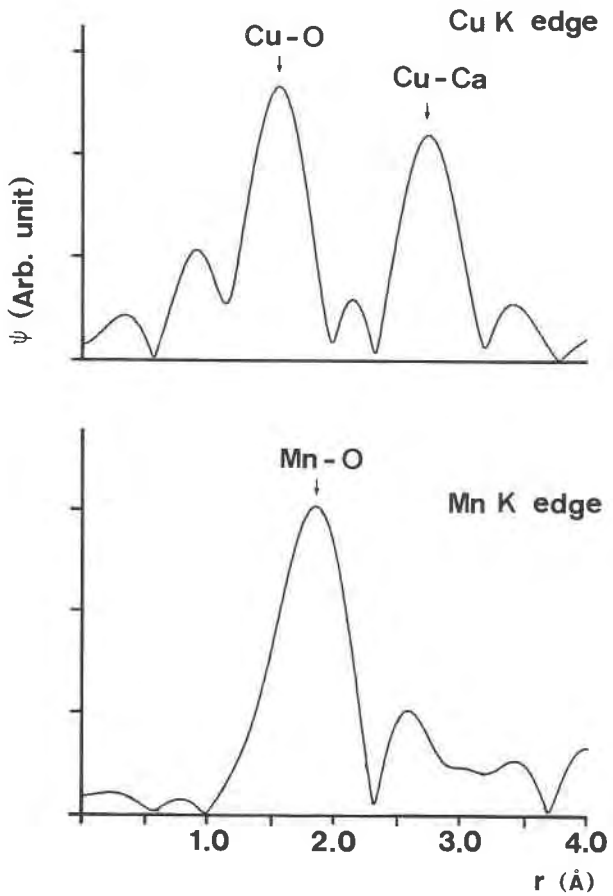

Fig. 3. Fourier transforms for the Cu*K* and Mn*K* edges. No phase shift correction is made.

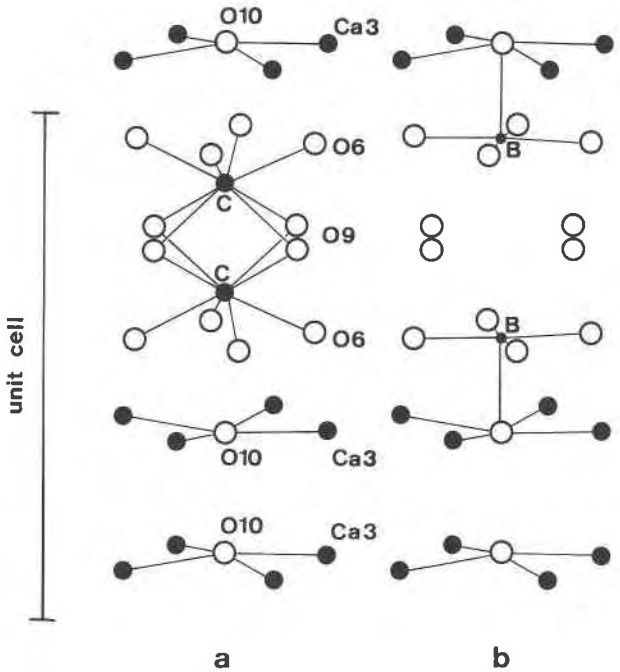

Fig. 4. Atomic arrangements along the fourfold axis that are not possible as cation-cation distances are too short (**a**) with only C sites occupied, (**b**) with only B sites occupied. The largest open circles represent O, intermediate solid circles Ca, and solid small circles Fe atoms.

Distribution of cations and F ions

Table 1 shows the number of ions per 50 cations in the four vesuvianite samples. The number of Si ions per formula unit (~18) indicates an almost total absence of $^{[4]}$Al. The Ca ions (with a few Na and K ions) sum to nearly 19; the substitution of Mn and other cations for Ca is not implied by these chemical analyses.

After several cycles of refinement, it was inferred that three Si (Si1, Si2, and Si3), four Ca (Ca1, Ca2, Ca3, and C), and one Al (A) sites are almost occupied by the Si, Ca, and Al ions, respectively. Consequently, the occupancy factors of these sites were constrained to the theoretical values in the final refinement. Occupancy factors for the B and AlFe sites are determined by two kinds of ions. In specimens 2 and 3, the B sites are occupied only by the Fe ions. Occupancy factors for O10 and O11 were refined using the atomic scattering factors of O and F, although those scattering factors are not significantly different. However, the refinements for specimens 2 and 3 suggest that the O10 positions are strongly occupied by F.

Figure 6 is a plot of effective ionic radius (*r*) (Shannon, 1976) vs. coordination number (CN), together with the average radius of cations occupying the fivefold-coordinated B sites and the octahedral AlFe sites. The average cation-anion interatomic distances for the octahedral A sites of the respective specimens (1.894, 1.897, 1.897, and 1.892 Å) suggest that the A sites are fully occupied only by Al. This is in agreement with the results obtained by Rucklidge et al. (1975) and Yoshiasa and Matsumoto (1986). The Al^{3+} ions preferentially occupy the A site rather than the AlFe site. Cation-anion interatomic distances for the AlFe site of specimen 1 are smaller than those of the others, and the occupancy factor (Table 3) indicates that the site contains none of higher atomic number than Al. This suggests that the AlFe site of specimen 1 is almost entirely occupied by Al (with minor Mg), i.e., all larger and higher atomic number atoms occupy the B site in specimen 1. The Zn ions of the Franklin copper vesuvianite sample are in the AlFe site, for which

Table 8. Interatomic distances determined by EXAFS (Å)

	Copper vesuvianite (Sauland)	Nakatatsu mine
One shell (fivefold)	Cu-O 1.98(1)	Mn-O 2.10(1)
	X-ray diffraction	
B-O6	2.063(3)	2.077(2)*
B-O10	2.199(6)	2.33(7)*
	Effective ionic radius**	
	$0.75(^{[5]}Mn^{2+}) + 1.38(^{[4]}O^{2-}) = 2.13$	
	$0.65(^{[5]}Cu^{2+}) + 1.38(^{[4]}O^{2-}) = 2.03$	

* Yoshiasa and Matsumoto (1986).
** Shannon (1976).

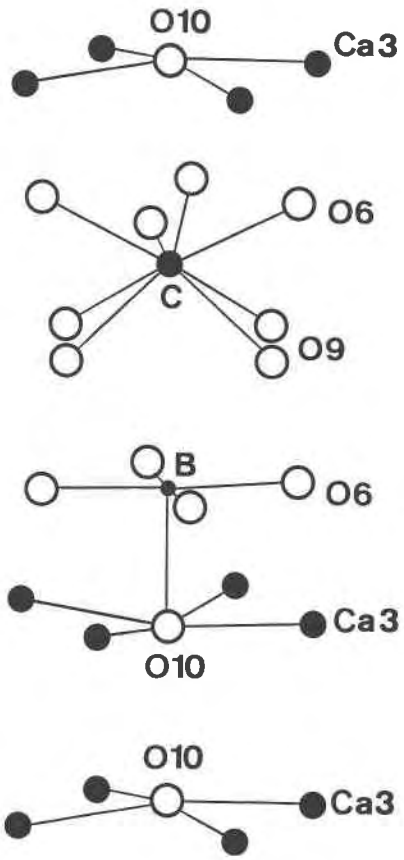

Fig. 5. Possible atomic arrangement along the fourfold axis. The symbols are the same as those in Figure 4.

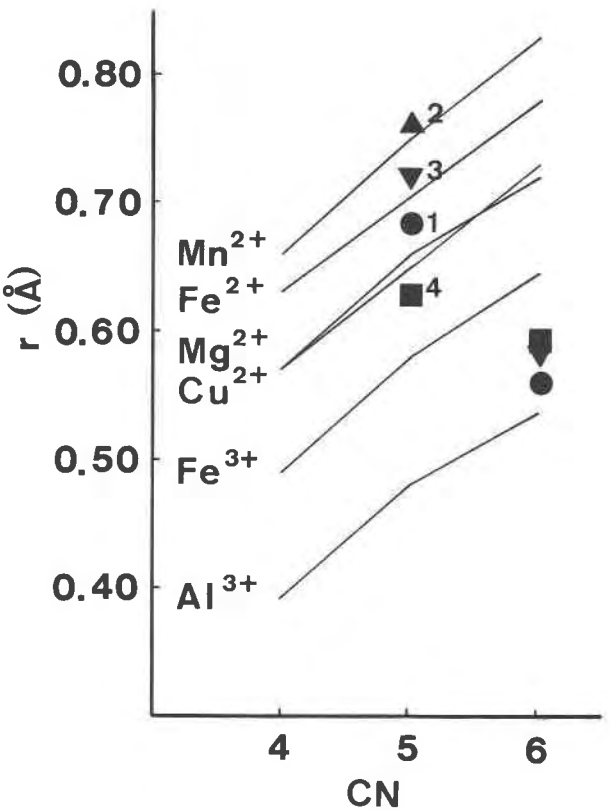

Fig. 6. Radii of cations that occupy the B site (fivefold coordinated) and the AlFe site (octahedral). Specimen numbers are the same as those in Table 1. Lines indicate the effective ionic radius (r) vs. coordination number (CN) (Shannon, 1976).

the average cation-anion interatomic distance is 1.954 Å (Fitzgerald et al., 1986a). The sizes of the fivefold-coordinated B sites are larger than those of the octahedral A and AlFe sites. In addition, variation in the size of the B sites in each specimen is greater than that of the other sites. Figure 6 and refined occupancy factors (Table 3) suggest that Fe and Cu ions occupy the B site in specimen 1. Valley et al. (1985) suggested that the B site is occupied by Mg in Fe-poor vesuvianite. The effective ionic radius of Mg^{2+} is almost the same as that of Cu^{2+}. Thus, the Cu ion should be able to occupy the B site. Comparison of Figure 6 and Table 3 leads to the conclusion that in specimens 2 and 3 the Fe ions are Fe^{2+} and in specimen 4, Fe^{3+}.

Local structure determined by EXAFS

Bond lengths around Cu in specimen 1 and Mn ions in the specimen from the Nakatatsu mine are listed in Table 8. The distance of first-shell ions from the Cu ion is 1.98(1) Å for specimen 1; the distance from the Mn ion is 2.10(1) Å for vesuvianite from Nakatatsu. Table 8 also lists the B-anion interatomic distances determined by structure refinement together with the effective ionic radii (Shannon, 1976). As is evident from Table 8, Cu and Mn ions occupy the fivefold-coordinated site. This result is the same as those of the refinements of specimens 1–4 and Fitzgerald et al. (1986a), which were obtained by single-crystal X-ray diffraction.

Structure variations around the B site

The polyhedron around the fivefold-coordinated B site is a square pyramid that has an O10 ion as an apex, the basal plane being formed by a square of four O6 ions. The B site is nearly at the center of this basal plane. The interatomic distances B-O6 and B-O10 for specimens 1–4 are 2.063, 2.087, 2.087, 2.038 Å and 2.199, 2.423, 2.278, 2.020 Å, respectively. Variation of the B-O10 distances is greater than that for B-O6. The volume of the square pyramid around the B site depends on the displacement of O10 along the fourfold axis. Displacements of O6 ions are relatively small because these anions are part of the silicate framework. The O10-O10 distances are 2.772, 2.400, 2.656, and 2.737 Å for specimens 1–4, respectively. The specimens with the shorter O10-O10 distances display larger values of the root-mean-square thermal displacements for B and O10 along the c axis (Table 9).

OH and F ions

OH ions occupy the O10 and O11 positions. The valence sums for anions of vesuvianite were calculated ac-

TABLE 9. Portion of root-mean-square thermal displacements along the **c** axis (Å)

	1 Sauland	2 Sanpo	3 Jinmu	4 Chichibu
C	0.125(1)	0.167(1)	0.152(1)	0.168(1)
B	0.183(1)	0.243(1)	0.244(1)	0.163(1)
O10	0.181(1)	0.373(1)	0.325(1)	0.217(1)

cording to the method of Donnay and Allmann (1970). The values of bond strengths of O1 through O9 of the respective specimens are approximately 2.0 and indicate that these sites are occupied by O ions. O11 is inferred to be occupied by OH because of the values 1.31, 1.40, 1.34, and 1.33 for specimens 1–4, respectively. The bond strengths for O10 of specimens 1–4 are 0.88, 0.79, 0.84, and 0.89 when the B site is unoccupied and 1.21, 0.87, 1.01, and 1.30 when the B site is occupied. These results are equivalent to those of previous studies (Giuseppetti and Mazzi, 1983; Yoshiasa and Matsumoto, 1986). In specimens 1–3, substitution of F for OH is confirmed by the results of the present chemical analyses (see Table 1). The O10 sites of specimens 2 and 3 are almost entirely occupied by F, and that of specimen 1 is occupied by nearly equal amounts of O and F ions (Table 3). Cation-anion distances (Table 6) suggest that the O10 site would be occupied by F when the O10-O10 distance is short. Figure 7 shows electron density maps of the four vesuvianite samples for the plane that passes through the C, B, and O10 sites at $y = 0.25$. The general shape of the electron density peaks for the C and B ions is normal, but that of O10 is abnormal. The shape of O10 in specimen 4 is less anomalous than those of the others, although there is a region of higher density between O10 ions. A difference Fourier synthesis of specimen 1 in the same plane is shown in Figure 8. In this part of the structure, it is difficult to determine the exact position of the H atom because there would be an adjustment in the O10 position under the influence of the surrounding cations. The O10-O10 interatomic distance of 2.772 Å is an appropriate distance for a linear H bond. The large electron density peaks in this difference Fourier map are presumed to correspond to the H atom. The height of the electron density peak is approximately 1.3 e/Å^3, and the distance from the O ion is approximately 1.07 Å. If the residual background is subtracted, the electron density peak of the H atom is approximately 0.6 e/Å^3. These values are also reasonable for H bonding. In non-*P*4/*nnc* vesuvianite structures, Giuseppetti and Mazzi (1983) and Fitzgerald et al. (1986b) suggest that H bonds exist between O10 atoms; i.e., the B site cation is bonded to O^{2-} and the C site cation to OH. In the difference map (Fig.

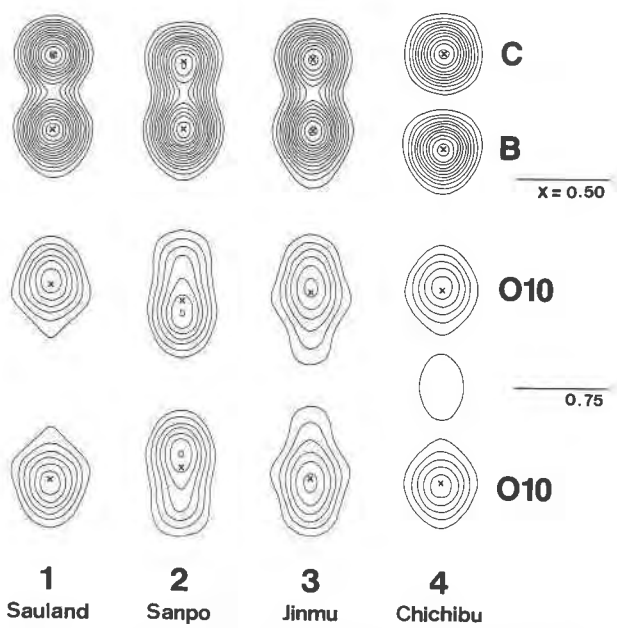

Fig. 7. Portion of the electron density maps of the four vesuvianite samples of this study in the plane that passes through the C, B, and O10 atoms. The location of these sites is indicated by ×. Contour starts from 5 e/Å^3 with interval of 5 e/Å^3.

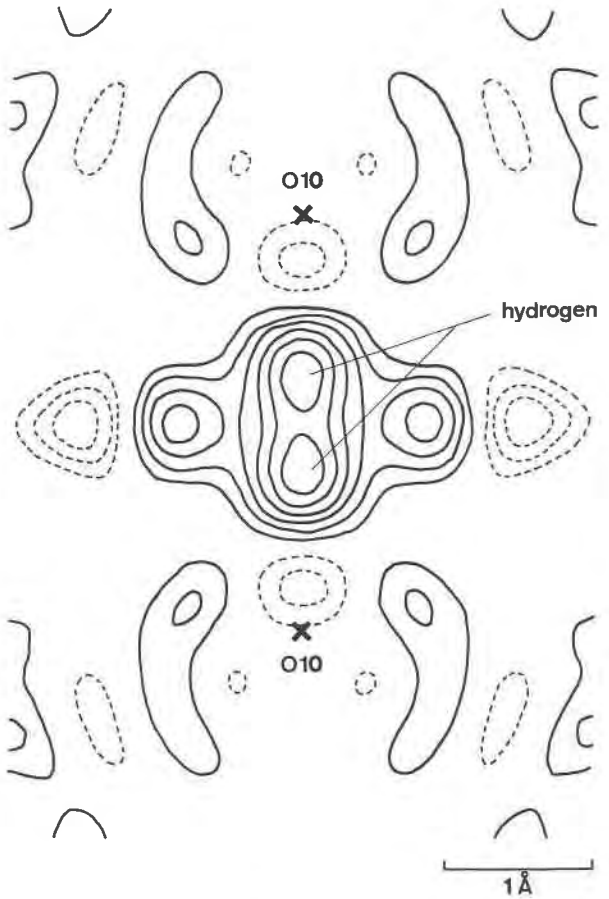

Fig. 8. Portion of the difference Fourier map of Sauland copper vesuvianite (specimen 1) in the plane that passes through the O10 ions. The location of the O10 sites is indicated by ×. Contours are drawn at an interval of 0.2 e/Å^3, zero contours being omitted and negative contours broken.

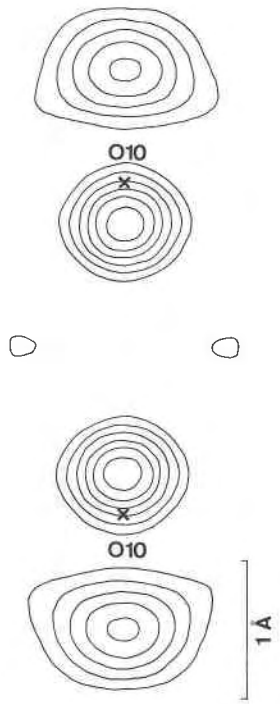

Fig. 9. Portion of the difference Fourier map of vesuvianite from the Sanpo mine (specimen 2) in the plane that passes through the O10 atoms. The location of the O10 sites is indicated by ×. Contour starts from 1.0 e/Å^3 with interval of 1.0 e/Å^3.

8), two peaks related by a twofold axis are evident. The H atoms statistically occupy one of these two positions.

In specimen 4, O10 is occupied almost entirely by O as the chemical analyses (Table 1) indicate little F. In the electron density map (Fig. 7), a high electron density region between both O10 positions is observed. It is not clear whether the electron density is that of H because of the higher R index. Data measurement for specimen 4 was carried out with a relatively weak incident X-ray beam (less than 25% of that for specimens 1 and 2). The higher R index for specimen 4 may be affected by the weak intensities. Therefore, the presence of a H atom could not be confirmed. However, the O10-O10 distance of 2.737 Å is suitable for H bonding. The results of bond valence calculations and chemical analysis suggest that H should bond to O10.

Abnormal displacement of O10 in specimen 2

The possibility of a lower symmetry is suggested for specimen 2; however, no violations of space group symmetry $P4/nnc$ were observed.

The anisotropic thermal parameter β_{11} (β_{22}) of O10 in specimen 2 became negative after several cycles of refinement. This parameter was therefore fixed at the refined value for vesuvianite from the Nakatatsu mine (Yoshiasa and Matsumoto, 1986). The O10 site in both of these vesuvianite crystals is entirely occupied by F.

O10 appears pear shaped in the electron density map (Fig. 7). In addition, the position of O10 does not coincide with the centroid of the electron density peak. The distance between the two O10 peaks is only about 2 Å (see Fig. 7), too short for O and F ions. In the difference Fourier map (Fig. 9), some residual electron density is evident. In contrast to specimen 2, the O10 positions in specimen 3, which has B and O10 positions occupied by Fe^{2+} and F^-, respectively, almost coincide with the centroid of the electron density peak. The electron density map features for Nakatatsu vesuvianite (Yoshiasa and Matsumoto, 1986) are intermediate to those of specimens 2 and 3. This can be interpreted as follows.

Rucklidge et al. (1975) pointed out that the B-site ion is almost coplanar with the square formed by four O6 atoms and so has greatest thermal displacement perpendicular to this plane. The O10 ion bonded to the B-site cation (the apex of the square pyramid) is almost coplanar with a square formed by four Ca3 cations. The root-mean-square thermal displacement of O10 along the fourfold axis is therefore quite similar to that of the B ion. The O10 atom adjacent to the C atom is fourfold coordinated because it is not bonded to the C atom, and thus it can vibrate more freely than O10, which is bonded to B. When O10 is O, an H atom is bonded to O10. However, when O10 is F, the F ion can vibrate more freely than an O ion because no H bond exists with the F ions. This displacement of the F ion is also correlated with the size of the square formed by four Ca3 atoms. The lengths of the edges of the Ca squares (Ca3-Ca3 distances) are 3.601, 3.696, 3.645, 3.595, and 3.663 Å for specimens 1–4 and Nakatatsu vesuvianite, respectively.

In specimen 2, Fe in the B site is almost entirely Fe^{2+}, and the O10 site is occupied by F^-. Thus, the B-O10 bond strength is smaller compared with that of Fe^{3+} and O^{2-}. In addition, the Ca3-O10 bond strength is rather small because of the large size of the Ca3 square. Fourfold-coordinated F near the C ion can be displaced more freely because no bonds to cations exist along the fourfold rotation axis. Therefore, O10 sites located near B and C ions violate the local twofold rotation symmetry. However, the ordering of cations along the fourfold axis would not occur. Thus, the average distribution of O10 ions produces a pear-shaped appearance on electron density maps that can be related to the difference between the two vibration ellipsoids. In the crystal structure of F-containing vesuvianite, the O10 site cannot be interpreted with a harmonic oscillation model.

Relationship between B-O10 and O10-O10 distances

Figure 10 shows the B-O10 vs. O10-O10 distances. Data are also taken from previous studies (Coda et al., 1970; Rucklidge et al., 1975; Giuseppetti and Mazzi, 1983; Valley et al., 1985; Fitzgerald et al., 1986a, 1986b; Yoshiasa and Matsumoto, 1986). Two vesuvianite samples (represented by open triangles) are non-$P4/nnc$ vesuvianite having the ordered structure along the fourfold rotation axis. H bonding is suggested in these vesuvianite samples (Giuseppetti and Mazzi, 1983; Fitzgerald et al., 1986b).

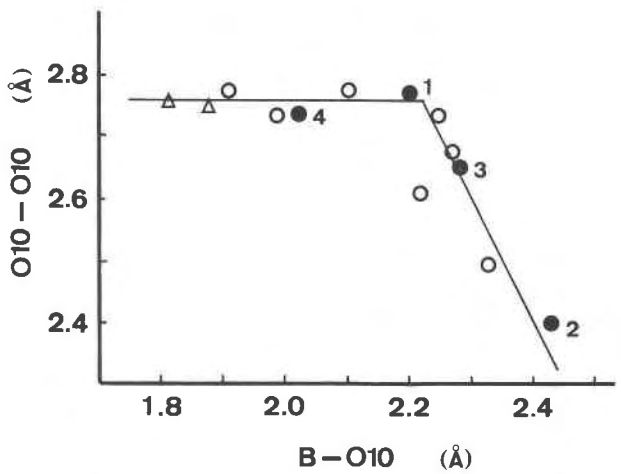

Fig. 10. O10-O10 distance vs. B-O10 distance. Solid circles = this study (specimen numbers are the same as those in Table 1); open circles = data from Coda et al. (1970), Rucklidge et al. (1975), Valley et al. (1985), Fitzgerald et al. (1986a), and Yoshiasa and Matsumoto (1986); triangles = (non-*P4/nnc* vesuvianite) data from Giuseppetti and Mazzi (1983) and Fitzgerald et al. (1986b).

In normal vesuvianite, when the O10-O10 distance is the same as that of non-*P4/nnc* vesuvianite, H bonding can exist. Relatively long B-O10 distances are recognized in specimens 2 and 3 and in vesuvianite from the Nakatatsu mine (Yoshiasa and Matsumoto, 1986); all of these contain F in O10. The longest B-O10 and the shortest O10-O10 distances are observed in specimen 2. In Figure 10, two groups can be recognized, one with B-O10 longer than 2.2 Å and the other shorter than 2.2 Å. In the group of longer B-O10 distances, the line in Figure 10 has a slope of −2.0 because displacements of O10-O10 are twice those of B-O10. For those vesuvianite samples with B-O10 < 2.2 Å, the displacement of O10-O10 distance is almost constant.

Acknowledgments

The authors express their sincere gratitude to Lawrence A. Taylor of University of Tennessee for his critical reading of the manuscript. Special thanks are due to Akira Kato of the National Science Museum and Chiyoko Henmi of Okayama University for providing the investigated samples. This work was performed under the approval of the Photon Factory Program Advisory Committee (proposal no. 88-135).

References cited

Coda, A., Della Giusta, A., Isetti, G., and Mazzi, F. (1970) On the crystal structure of vesuvianite. Atti Della Accademia Delle Scienze Di Torino, 105, 63–84.

Deer, W.A., Howie, R.A., and Zussman, J. (1982) Rock-forming minerals, vol. 1A: Orthosilicates (2nd edition), 699–718. Longman, London.

Donnay, G., and Allmann, R. (1970) How to recognize O^{2-}, OH^-, and H_2O in crystal structures determined by X-rays. American Mineralogist, 55, 1003–1015.

Finger, L.W. (1969) Determination of cation distribution by least-squares refinement of single-crystal X-ray data. Carnegie Institution of Washington Year Book, 67, 216–217.

Fitzgerald, S., Rheingold, A.L., and Leavens, P.B. (1986a) Crystal structure of a Cu-bearing vesuvianite. American Mineralogist, 71, 1011–1014.

——— (1986b) Crystal structure of a non-*P4/nnc* vesuvianite from Asbestos, Quebec. American Mineralogist, 71, 1483–1488.

Fitzgerald, S., Leavens, P.B., Rheingold, A.L., and Nelen, J.A. (1987) Crystal structure of a REE-bearing vesuvianite from San Benito County, California. American Mineralogist, 72, 625–628.

Giuseppetti, G., and Mazzi, F. (1983) The crystal structure of a vesuvianite with *P4/n* symmetry. Tschermaks mineralogische und petrographische Mitteilungen, 31, 277–288.

Ibers, J.A., and Hamilton, W.C., Eds. (1974) International tables for X-ray crystallography, vol. 4, p. 71–147. Kynoch Press, Birmingham, England.

Ito, J., and Arem, J.E. (1970) Idocrase: Synthesis, phase relations and crystal chemistry. American Mineralogist, 55, 880–912.

Lager, G.A., Xie, Q., Ross, F.K., Rossman, G.R., Armbruster, T., Rotella, F.J., and Schultz, A.J. (1989) Crystal structure of a *P4/nnc* vesuvianite from Tanzania, Africa. Geological Society of America Abstracts with Programs, 21, A120.

Maeda, H. (1987) Accurate bond length determination by EXAFS method. Journal of the Physical Society of Japan, 56, 2777–2787.

Neuman, H., and Svinndal, S. (1955) The cyprine-thulite deposit at Ovstebo near Kleppan in Sauland, Telemark. Norsk Geologisk Tidsskrift, 34, 139–156.

Phillips, B.L., Allen, F.M., and Kirkpatrick, R.J. (1987) High-resolution solid-state ^{27}Al NMR spectroscopy of Mg-rich vesuvianite. American Mineralogist, 72, 1190–1194.

Rucklidge, J.C., Kocman, V., Whitlow, S.H., and Gabe, E.J. (1975) The crystal structures of three Canadian vesuvianites. Canadian Mineralogist, 13, 15–21.

Shannon, R.D. (1976) Revised effective ionic radii and systematic studies of interatomic distances in halides and chalcogenides. Acta Crystallographica, A32, 751–767.

Teo, B.-K., and Lee, P.A. (1979) Ab initio calculations of amplitude and phase functions for extended X-ray absorption fine structure spectroscopy. Journal of the American Chemical Society, 101, 2815–2832.

Valley, J.W., Peacor, D.R., Bowman, J.R., Essene, E.J., and Allard, M.J. (1985) Crystal chemistry of a Mg-vesuvianite and implications of phase equilibria in the system CaO-MgO-Al_2O_3-SiO_2-H_2O-CO_2. Journal of Metamorphic Geology, 3, 137–153.

Warren, B.E., and Modell, D.I. (1931) The structure of vesuvianite $Ca_{10}Al_4(Mg,Fe)_2Si_9O_{34}(OH)_4$. Zeitschrift für Kristallographie, 78, 422–432.

Yoshiasa, A., and Matsumoto, T. (1986) The crystal structure of vesuvianite from Nakatatsu mine: Reinvestigation of the cation site-populations and of the hydroxyl groups. Mineralogical Journal, 13, 1–12.

Yoshiasa, A., Inoue, Y., Kanamaru, F., and Koto, K. (1990a) Local structure and spin state of Co^{4+} ions in the perovskite-type $SrCo_{1-x}Mn_xO_3$ solid-solution. Journal of Solid State Chemistry, 86, 75–81.

Yoshiasa, A., Maeda, H., Ishii, T., and Koto, K. (1990b) EXAFS studies on anharmonic thermal vibrations in AgI. Solid State Ionics, 40–41, 341–344.

Manuscript received October 2, 1991
Manuscript accepted May 11, 1992